Journal of Organometallic Chemistry, 250 (1983) 237–246
Elsevier Sequoia S.A., Lausanne – Printed in The Netherlands

ACTINIDE-CENTERED CYCLOMETALATION CHEMISTRY. AN UNUSUALLY DISTORTED THORIUM BISHYDROCARBYL: $Th[\eta^5-(CH_3)_5C_5]_2[CH_2Si(CH_3)_3]_2$

JOSEPH W. BRUNO, TOBIN J. MARKS *,

Department of Chemistry, Northwestern University, Evanston, Illinois 60201 (U.S.A.)

and VICTOR W. DAY *

Department of Chemistry, University of Nebraska, Lincoln, Nebraska, 68588 and Crystalytics Company, Lincoln, Nebraska, 68501 (U.S.A.)

(Received January 4th, 1983)

Summary

The crystal and molecular structure of the complex $Th[\eta^5-(CH_3)_5C_5]_2[CH_2Si(CH_3)_3]_2$, which undergoes facile intramolecular cyclometalation to the thoracyclobutane $Th[\eta^5-(CH_3)_5C_5]_2(CH_2)_2Si(CH_3)_2$, is reported. While the $Th[\eta^5-(CH_3)_5C_5]_2$ ligation is unexceptional, the $Th[CH_2Si(CH_3)_3]_2$ fragment is highly unsymmetrical having Th–C (corresponding angle Th–C–Si) 2.51(1) Å (132.0(6)°) and 2.46(1) Å (148.0(7)°). This conformation, which appears to result from severe intramolecular non-bonded contacts, allows a methyl hydrogen atom of one $CH_2Si(CH_3)_3$ ligand to approach within ca. 2.3 Å of the α-carbon atom of the other $CH_2Si(CH_3)_3$ ligand.

Introduction

Metal-mediated processes that result in the scission of two-center, two-electron (2*c*,2*e*) H–H and C–H bonds are of fundamental significance in hydrocarbon catalysis and in devising new strategies for selective, stoichiometric hydrocarbon activation [1–7]. In earlier work [8] we presented examples where bis(pentamethylcyclopentadienyl)-organoactinides of the formula Cp'_2MR_2 ($Cp' = \eta^5-(CH_3)_5C_5$; M = Th, U; R = hydrocarbyl) effected the cleavage of H–H and aromatic C–H bonds with surprising facility. Mechanistic proposals based upon accessible actinide oxidation states [9] stressed the importance of "four-center" "heterolytic" activation processes (e.g., eq. 1) [10] which do not require formal oxidative addition/reductive

---

* To whom correspondence should be addressed.

0022-328X/83/$03.00

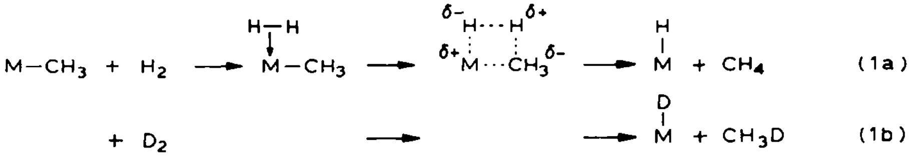

$$M-CH_3 + H_2 \longrightarrow \overset{H-H}{\overset{\downarrow}{M}}-CH_3 \longrightarrow \begin{matrix} \overset{\delta-}{H}\cdots\overset{\delta+}{H} \\ \vdots \qquad \vdots \\ \overset{\delta+}{M}\cdots\overset{\delta-}{CH_3} \end{matrix} \longrightarrow \overset{H}{\overset{|}{M}} + CH_4 \qquad (1a)$$

$$+ D_2 \longrightarrow \qquad \longrightarrow \overset{D}{\overset{|}{M}} + CH_3D \qquad (1b)$$

elimination, and which are plausibly accelerated by the high actinide electrophilicity and coordinative unsaturation. In an effort to further define those modes of 2*c*,2*e* bond activation which can occur about actinide centers and to compare/contrast the pathways with those at transition metal centers, we have now turned our attention to C–H activation involving saturated hydrocarbons.

Capitalizing first upon the 10^5–10^6-fold kinetic advantage that accrues in optimal intramolecular processes, we have studied the thermolysis of the organothorium compounds $Cp_2'Th[CH_2Si(CH_3)_3]_2$ (I) and $Cp_2'Th[CH_2C(CH_3)_3]_2$ (II) [11]. These bishydrocarbyls undergo clean, kinetically unimolecular decomposition to yield the corresponding thoracyclobutanes III and IV, respectively (eqs. 2, 3). Mechanistic arguments based upon deuterium labelling, activation parameters ($\Delta S^{\neq}$ is negative), and plausibly accessible thorium oxidation states, suggest again a four-center, heterolytic activation process (V) in apparent contrast to known Group VIII chemistry [5–7, 2–6]. It would be of obvious interest to establish a structural basis

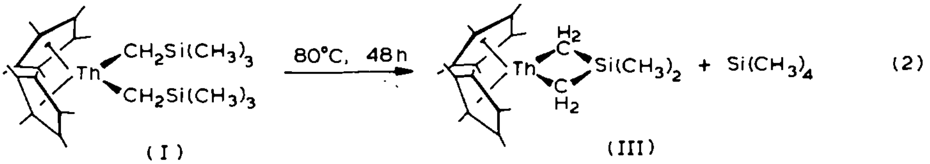

(I) (III)

(2)

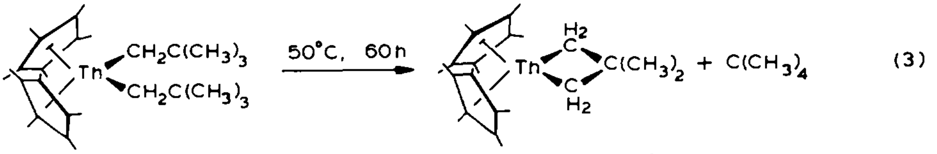

(II) (IV)

(3)

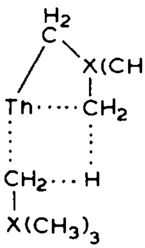

(V, X = C, Si)

for further organoactinide mechanistic discussion. In reference [11] we report the molecular structure of thoracyclobutane III and show the $Th(CH_2)_2SiC_2$ fragment to have approximate C_{2v} symmetry, with the only significant deviation being a 6° folding of the metallacycle along the CH_2–CH_2 vector to relieve non-bonded interactions between $Si(CH_3)_2$ and ring methyl groups. In the present contribution, we focus upon the molecular structure of the precursor complex I, which features some surprising and suggestive distortions.

Experimental

The complex $Cp_2'Th[CH_2Si(CH_3)_3]_2$ (I) was synthesized as described in reference [8]. Large, well-shaped single crystals were obtained by slow cooling (room temperature to −30°C) of saturated heptane solutions. The crystals are, at 20 ± 1°C, monoclinic, space group $P2_1/n$ (an alternate setting of $P2_1/c$-C_{2h}^5, No. 14 [17]) with a 10.125(3), b 30.789(7), c 11.002(4) Å, β 111.56(2)°, V 3190(2) Å^3, and $Z = 4$ (μ_a(Mo-$K_{\bar{\alpha}}$) [18] 4.92 mm^{-1}; d_{calc} 1.410 g cm^{-3}).

Intensity measurements were made on a Nicolet P$\bar{1}$ autodiffractometer using 0.90°-wide ω scans and graphite-monochromated Mo-$K_{\bar{\alpha}}$ radiation for a specimen having the shape of a rectangular parallelepiped with dimensions of 0.38 × 0.48 × 0.60 mm. This crystal was sealed under N_2 in a thin-walled glass capillary and mounted on a goniometer with its longest dimension nearly parallel to the φ-axis of the diffractometer. A total of 7335 independent reflections having $2\theta_{\text{Mo-}K_{\bar{\alpha}}} < 55.0°$ (the equivalent of 1.0 limiting Cu-$K_{\bar{\alpha}}$ spheres) were measured in two concentric shells of 2θ. A scanning rate of 6° min^{-1} was used to measure intensities for reflections having $3° \leqslant 2\theta \leqslant 43°$ and a rate of 4° min^{-1} for the remaining reflections. The data collection and reduction procedures which were used are described elsewhere [21]; the scan width and step-off for background measurements were both 0.90° and the ratio of total background counting time to net scanning time was 0.50. The intensity data were corrected empirically for absorption effects using ψ-scans for six reflections having 2θ between 9 and 29° (the relative transmission factors ranged from 0.63 to 1.00).

The structure was solved using the "heavy-atom" technique. Unit-weighted anisotropic full-matrix least-squares refinement of the parameters for the Th and two Si atoms converged to R_1 (unweighted, based on F) = 0.138 and R_2 (weighted, based on F) = 0.185 for 2606 independent reflections having $2\theta_{\text{Mo-}K_{\bar{\alpha}}} < 43°$ and $I > 3\sigma(I)$ [22]. Inclusion of the remaining 28 nonhydrogen atoms into the model with anisotropic thermal parameters gave $R_1 = 0.040$ and $R_2 = 0.046$ for 2606 unit-weighted reflections. Hydrogen atoms could not be located from a difference Fourier calculated at this point.

The final cycles of empirically-weighted [23] full-matrix least-squares refinement which utilized the more complete ($2\theta_{\text{Mo-}K_{\bar{\alpha}}} < 55°$) data set and anisotropic thermal parameters for all nonhydrogen atoms gave $R_1 = 0.048$ and $R_2 = 0.054$ for 4247 independent absorption-corrected reflections having $I > 3\sigma(I)$. Since a careful comparison of final $|F_0|$ and $|F_c|$ values indicated the absence of extinction effects, extinction corrections were not made.

All structure factor calculations employed recent tabulations of atomic form factors [19] and anomalous dispersion corrections [20] to the scattering factors of the Th and Si atoms. All calculations were performed on a Data General Eclipse S-200 computer equipped with 64K of 16-bit words, a floating point processor for 32- and 64-bit arithmetic and versions of the Nicolet EXTL interactive crystallographic software package as modified at Crystalytics Company.

Results and discussion

The X-ray structural analysis reveals that single crystals of I are composed of discrete mononuclear $Th[\eta^5\text{-}(CH_3)_5C_5]_2[CH_2Si(CH_3)_3]_2$ molecules such as shown

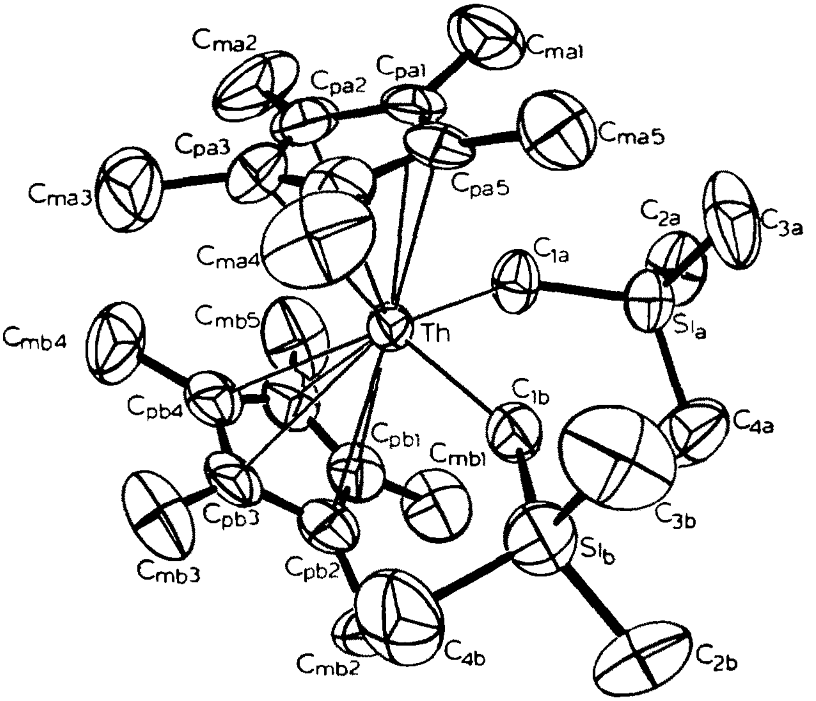

Fig. 1. Perspective ORTEP drawing of the Th[η^5-$(CH_3)_5C_5]_2[CH_2Si(CH_3)_3]_2$ molecule (I) viewed nearly along the plane of the equatorial girdle. All nonhydrogen atoms are represented by thermal vibration ellipsoids drawn to encompass 50% of the electron density.

in Figs. 1 and 2. The Th^{IV} ion adopts the familiar "bent sandwich" Cp'_2MX_2 actinide coordination geometry [9,21,24], being π-bonded to two $(CH_3)_5C_5^-$ ligands and σ-bonded to two $CH_2Si(CH_3)_3^-$ ligands. Final atomic coordinates and anisotropic thermal parameters for nonhydrogen atoms of crystalline I are presented in Tables 1 and 2 *, respectively. Bond lengths and angles involving nonhydrogen atoms of I are given in Table 3. The atom labeling scheme is shown in Fig. 1.

Turning first to the η^5-$(CH_3)_5C_5$ ligation, it can be seen that the intraligand metrical parameters are not exceptional for a Cp'_2ThX_2 complex [9,11,21,24]. Thus, the C_5 rings are coplanar to within 0.010 Å [25,26], while the methyl groups are displaced 0.073–0.264 Å from the C_5 mean plane in a direction away from the thorium ion. In each ring, the methyl groups closest to the plane defined by the C_{1a}–Th–C_{1b} "equatorial girdle" i.e., carbon atoms C_{ma3} and C_{mb4}, exhibit the largest displacement ($>$ 0.24 Å). The average C–C distance of 1.41 (2,2,4,10) Å [27], Th–C distance of 2.81 (1,1,4,10) Å [27], and C–CH_3 distance of 1.53 (2,2,3,10) Å [27] are typical values for η^5-$(CH_3)_5C_5$ bonding [9,11,21,24,28–30]. Moreover, the present (ring-center-of-gravity)–Th–(ring-center-of-gravity) angle of 134.9° compares favorably to values of 138, 138, 129, 138.5, and 130° in $Cp'_2Th(Cl)[\eta^2$-

---

* *Supplementary material available.* A table of fractional atomic coordinates (Table 1), a table of anisotropic thermal parameters for nonhydrogen atoms (Table 2), detailed experimental descriptions of the X-ray crystallographic studies, and structure factor tables will be provided by the authors upon request.

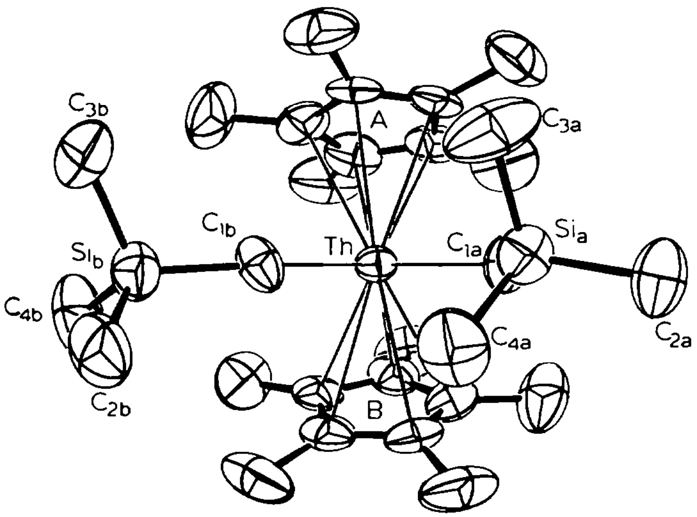

Fig. 2. Perspective ORTEP drawing of the $Th[\eta^5\text{-}(CH_3)_5C_5]_2[CH_2Si(CH_3)_3]_2$ molecule (I) viewed nearly along the bisector of the C_{1a}–Th–C_{1b} angle. All nonhydrogen atoms are represented by thermal vibration ellipsoids drawn to encompass 50% of the electron density.

TABLE 3

BOND LENGTHS AND ANGLES INVOLVING NONHYDROGEN ATOMS IN CRYSTALLINE $Th[\eta^5\text{-}(CH_3)_5C_5]_2[CH_2Si(CH_3)_3]_2$[a]

Type[b]	Length (Å)	Type[b]	Length (Å)
$Th-C_{pa1}$	2.82(1)	$C_{pa1}-C_{pa2}$	1.41(2)
$Th-C_{pa2}$	2.80(1)	$C_{pa1}-C_{pa5}$	1.38(2)
$Th-C_{pa3}$	2.77(1)	$C_{pa2}-C_{pa3}$	1.43(2)
$Th-C_{pa4}$	2.79(1)	$C_{pa3}-C_{pa4}$	1.39(2)
$Th-C_{pa5}$	2.80(1)	$C_{pa4}-C_{pa5}$	1.42(2)
$Th-C_{pb1}$	2.80(1)	$C_{pb1}-C_{pb2}$	1.39(2)
$Th-C_{pb2}$	2.82(1)	$C_{pb1}-C_{pb5}$	1.38(2)
$Th-C_{pb3}$	2.82(1)	$C_{pb2}-C_{pb3}$	1.45(2)
$Th-C_{pb4}$	2.83(1)	$C_{pb3}-C_{pb4}$	1.43(2)
$Th-C_{pb5}$	2.81(1)	$C_{pb4}-C_{pb5}$	1.41(2)
$Th-C_{ga}$[c]	2.53(-)	$C_{pa1}-C_{ma1}$	1.55(2)
$Th-C_{gb}$[c]	2.55(-)	$C_{pa2}-C_{ma2}$	1.51(2)
		$C_{pa3}-C_{ma3}$	1.53(2)
$Th-C_{1a}$	2.51(1)	$C_{pa4}-C_{ma4}$	1.53(2)
$Th-C_{1b}$	2.46(1)	$C_{pa5}-C_{ma5}$	1.55(2)
Si_a-C_{1a}	1.86(1)	$C_{pb1}-C_{mb1}$	1.56(2)
Si_a-C_{2a}	1.88(2)	$C_{pb2}-C_{mb2}$	1.51(3)
Si_a-C_{3a}	1.88(2)	$C_{pb3}-C_{mb3}$	1.50(2)
Si_a-C_{4a}	1.89(2)	$C_{pb4}-C_{mb4}$	1.51(2)
		$C_{pb5}-C_{mb5}$	1.54(2)
Si_b-C_{1b}	1.87(1)		
Si_b-C_{2b}	1.86(2)		
Si_b-C_{3b}	1.89(2)		
Si_b-C_{4b}	1.87(2)		

Table 3 (continued)

Type [b]	Angle (deg.)	Type [b]	Angle (deg.)
$C_{ga}ThC_{gb}$ [c]	134.9(-)	$C_{1a}ThC_{1b}$	96.8(4)
$C_{ga}ThC_{1a}$ [c]	103.7(-)	$ThC_{1a}Si_a$	132.0(6)
$C_{ga}ThC_{1b}$ [c]	106.1(-)	$ThC_{1b}Si_b$	148.0(7)
$C_{gb}ThC_{1a}$ [c]	102.2(-)		
$C_{gb}ThC_{1b}$ [c]	106.8(-)		
$C_{1a}Si_aC_{2a}$	108.9(7)	$C_{1b}Si_bC_{2b}$	111.4(8)
$C_{1a}Si_aC_{3a}$	111.8(7)	$C_{1b}Si_bC_{3b}$	110.6(8)
$C_{1a}Si_aC_{4a}$	114.2(7)	$C_{1b}Si_bC_{4b}$	114.4(8)
$C_{2a}Si_aC_{3a}$	108.5(8)	$C_{2b}Si_bC_{3b}$	107.4(9)
$C_{2a}Si_aC_{4a}$	106.4(8)	$C_{2b}Si_bC_{4b}$	106.0(9)
$C_{3a}Si_aC_{4a}$	106.9(8)	$C_{3b}Si_bC_{4b}$	106.8(9)
$C_{pa2}C_{pa1}C_{pa5}$	109(1)	$C_{pb2}C_{pb1}C_{pb5}$	110(1)
$C_{pa1}C_{pa2}C_{pa3}$	105(1)	$C_{pb1}C_{pb2}C_{pb3}$	107(1)
$C_{pa2}C_{pa3}C_{pa4}$	110(1)	$C_{pb2}C_{pb3}C_{pb4}$	107(1)
$C_{pa3}C_{pa4}C_{pa5}$	107(1)	$C_{pb3}C_{pb4}C_{pb5}$	107(1)
$C_{pa4}C_{pa5}C_{pa1}$	109(1)	$C_{pb4}C_{pb5}C_{pb1}$	109(1)
$C_{pa2}C_{pa1}C_{ma1}$	124(1)	$C_{pb2}C_{pb1}C_{mb1}$	123(1)
$C_{pa5}C_{pa1}C_{ma1}$	126(1)	$C_{pb5}C_{pb1}C_{mb1}$	127(1)
$C_{pa1}C_{pa2}C_{ma2}$	124(1)	$C_{pb1}C_{pb2}C_{mb2}$	128(1)
$C_{pa3}C_{pa2}C_{ma2}$	130(1)	$C_{pb3}C_{pb2}C_{mb2}$	125(1)
$C_{pa2}C_{pa3}C_{ma3}$	124(1)	$C_{pb2}C_{pb3}C_{mb3}$	128(1)
$C_{pa4}C_{pa3}C_{ma3}$	125(1)	$C_{pb4}C_{pb3}C_{mb3}$	125(1)
$C_{pa3}C_{pa4}C_{ma4}$	127(1)	$C_{pb3}C_{pb4}C_{mb4}$	126(1)
$C_{pa5}C_{pa4}C_{ma4}$	127(1)	$C_{pb5}C_{pb4}C_{mb4}$	126(1)
$C_{pa4}C_{pa5}C_{ma5}$	124(1)	$C_{pb4}C_{pb5}C_{mb5}$	125(1)
$C_{pa1}C_{pa5}C_{ma5}$	127(1)	$C_{pb1}C_{pb5}C_{mb5}$	125(1)

[a] The numbers in parentheses are the estimated standard deviations in the last significant digit. [b] Atoms are labeled in agreement with Tables 1 and 2 and Fig. 1. [c] C_{ga} and C_{gb} refer to centers of gravity for the five-carbon rings of pentamethylcyclopentadienyl ligands *a* and *b*, respectively.

$CON(C_2H_5)_2]$ [21], $Cp'_2Th(Cl)[\eta^2\text{-}COCH_2C(CH_3)_3]$ [31], $\{Cp'_2Th[O_2C_2(CH_3)_2]\}_2$ [32] (III) [11], and $(Cp'_2ThH_2)_2$ [33], respectively. Even with the two $(CH_3)_5C_5^-$ ligands in I adopting a nearly staggered configuration, several intramolecular nonbonded methyl ··· methyl contacts between $(CH_3)_5C_5^-$ ligands are still slightly (0.10–0.15 Å) less than the 4.00 Å Van der Waals diameter [34] of a methyl group, and the C_{ma3} ··· C_{mb4} contact (3.44 Å) is only 0.04 Å larger than the 3.40 Å Van der Waals diameter [34] of carbon. The C_{1a}–Th–C_{1b} "equatorial girdle" mean plane [35] intersects the C_{ga}–Th–C_{gb} mean plane [36] in a dihedral angle of 89.2°. The least-squares mean planes [25,26] for the C_5 rings of Cp′ ligands A and B intersect the C_{ga}–Th–C_{gb} mean plane in dihedral angles of 89.2 and 89.9°, respectively, and that of the "equatorial girdle" in angles of 23.8 and 22.0°, respectively. This situation is again typical of a Cp'_2ThX_2 complex.

As concerns the $Th[CH_2Si(CH_3)_3]_2$ coordination, the C_{1a}–Th–C_{1b} angle of 96.8(4)° is not unexpected [11,21,24]. However, the exact disposition of the hydrocarbyl ligands about the Th^{IV} ion is unusual, and results in a marked deviation from the approximate C_{2v} symmetry (assuming eclipsed cyclopentadienyl rings) normally observed for typical transition metal Cp_2MX_2 [37,38] and actinide Cp'_2MX_2 [11,21,24,39] complexes. To aid in describing this distortion, we define a Cartesian coordinate system (VI) which is centered at the metal ion and has the x axis at the intersection of the "equatorial girdle" and the C_{ga}–Th–C_{gb} mean plane. Under idealized C_{2v} symmetry, the x axis would coincide with the required twofold axis. The y axis lies in the "equatorial girdle" parallel to both C_5 ring mean planes. Importantly, unlike the distribution of X ligands in most other Cp_2MX_2 complexes [37,38], carbon atoms C_{1a} and C_{1b} in I are not symmetrically disposed about the x axis. Rather, C_{1a} is displaced by 2.04 Å from the C_{ga}–Th–C_{gb} plane in the positive y direction, while C_{1b} is displaced by only 1.66 Å in the negative y direction. In contrast, we find the closely related thorium dialkyl $Cp'_2Th(CH_3)_2$ to exhibit a completely symmetrical arrangement in the "equatorial girdle" and, in fact, to possess rigorous C_{2v} symmetry in the solid state [39].

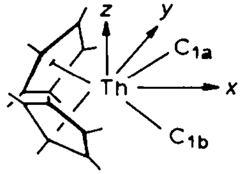

(VI)

The exact coordination of the trimethylsilylmethyl ligands in I is also rather unsymmetrical. The Th–C_{1a}–Si_a angle of 132.0(6)°, while significantly larger than tetrahedral, has precedent in the molecular structures of other organoactinide hydrocarbyls. Corresponding M–C–C angles in other compounds are 128.5(16)° in Cp_3U(n-butyl) [40] and 128.6(9)° in $Cp_3U(CH_2$-p-$C_6H_4CH_3)$ [40]. While no 5f trimethylsilylmethyl crystal structures have been reported, the M–C–Si angle in $Cp_2LuCH_2Si(CH_3)_3 \cdot THF$ is 130.7(8)° [41]. In contrast, the Th–C_{1b}–Si_b angle in I of 148.0(7)° is, to our knowledge unprecedented for a d- or f-element hydrocarbyl involving a monohapto, sp^3 carbon atom. In regard to Th–C σ bond lengths, it can be seen (Table 3) that Th–C_{1a} and Th–C_{1b} are significantly different (2.51(1) vs. 2.46(1) Å), with the shorter distance being associated with the unusually obtuse Th–C–Si angle. For comparison, the corresponding distances in III (with Th–C–Si angles of 90.6 (5,5,5,2)°) are 2.463(13) and 2.485(14) Å [11], meaning that comparably "short" distances are associated in this case with rather acute Th–C–Si angles. For this reason, we are reluctant at this stage to read any significance into the shorter Th–C_{1b} contact in I. The metrical parameters, within the $CH_2Si(CH_3)_3$ ligands of I are unexceptional [41]: the Si–C bond lengths range from 1.86(2) to 1.89(2) Å and the C–Si–C angles range from 106(1) to 114(1)° with an average value of 109 (1,3,5,12)°.

Defining the Th–C_{1a} and Th–C_{1b} bonds as axes of rotation and the bisectors of the Th–C–Si angles as vectors, it can be seen in Figs. 1 and 2 that there are basically three extreme orientations of the vectors: (i) pointing toward each other, (ii) pointing away from each other, (iii) pointing in the same general y axis direction (as observed). For all but very compact alkyl moieties, inspection of a diffraction-derived molecular model reveals that while conformation (iii) involves some distortion of the Th–$CH_2Si(CH_3)_3$ bonding and several short non-bonded contacts (vide infra), it still best minimizes nonbonded repulsions. Thus, beginning in conformation (iii), the model indicates that rotation about the Th–C_{1a} bond by up to 180°, results in unacceptably close non-bonded methyl–methyl contacts with the $(CH_3)_5C_5^-$ ligands [42]. Likewise, rotation about the Th–C_{1b} bond by up to 180° produces unacceptably short non-bonded methyl–methyl contacts with the other $CH_2Si(CH_3)_3$ ligand. The best compromise thus appears to be conformation (iii) which, while not possessing unacceptable non-bonded contacts, is nevertheless somewhat crowded. Close contacts involving the $CH_2Si(CH_3)_3$ and η^5-$(CH_3)_5C_5$ ligands include: $C_{4b} \cdots C_{mb2}$, 3.76 Å; $C_{1a} \cdots C_{ma1}$, 3.43 Å; $C_{1a} \cdots C_{mb1}$, 3.52 Å; $C_{1a} \cdots C_{mb5}$, 3.69 Å; $C_{1b} \cdots C_{ma4}$, 3.81 Å; $C_{1b} \cdots C_{ma5}$, 3.66 Å; $C_{1b} \cdots C_{mb2}$, 3.49 Å. Between the two $CH_2Si(CH_3)_3$ ligands, $C_{1a} \cdots C_{1b}$ 3.71(2) Å is also rather short. Also of possible chemical significance is the spatial relationship of C_{4a} and its attached hydrogen atoms to C_{1b}. The crystal structure reveals the $C_{4a} \cdots C_{1b}$ distance to be 3.97 Å, and inspection of a diffraction-derived scale model indicates that a modest rotation about bond C_{1a}–Si_a brings C_{4a} to within ca. 3.4 Å of C_{1b}. Assuming a C–H bond distance of 1.09 Å [43], subsequent rotation about bond Si_a–C_{4a} can bring a methyl hydrogen atom on C_{4a} to within ca. 2.3 Å of C_{1b}–fully 0.8 Å shorter than the sum of the C and H Van der Waals radii [34]. A similar exercise with carbon atoms C_{ma1} and C_{mb1} brings the methyl hydrogen atoms to within ca. 2.7 Å of C_{1a}.

Conclusions

The results of the present structural analysis indicate that while the bis(pentamethylcyclopentadienyl) ligation in $Cp'_2Th[CH_2Si(CH_3)_3]_2$ is not unusual, the remainder of the molecular geometry appears to be heavily influenced by significant intramolecular non-bonded interactions. Of the possible ground state $Th[CH_2Si(CH_3)_3]_2$ conformations, it should be noted that the one observed would be a plausible configuration along the cyclometalation reaction coordinate illustrated in eq. 4. Interestingly, the possibility that the $C_{1b} \cdots C_{4a}$ type of interaction involves a major perturbation of the H–C_{4a} bond and that it represents a deep minimum on the conformational potential energy surface are not confirmed by spectroscopic data: neither the infrared spectrum nor the 270 MHz ^1H NMR down to −95°C indicate unusual bonding or conformational energetics [45]. Further conclusions await X-ray diffraction studies of II (which should be even more crowded) as well as neutron diffraction studies of both I and II.

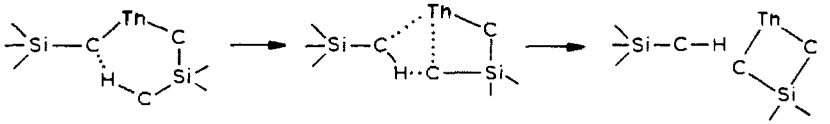

(4)

Acknowledgment

This research was generously supported by the National Science Foundation (Grant CHE8009060 to TJM).

References

1 C. Masters, Homogeneous Transition-Metal Catalysis, Chapman and Hall, London, 1981.

2 H. Pines, The Chemistry of Catalytic Hydrocarbon Conversions, Academic Press, New York, 1981.

3 G.W. Parshall, Homogeneous Catalysis, Wiley-Interscience, New York, 1980.

4 J.P. Collman and L.S. Hegedus, Principles and Applications of Organotransition Metal Chemistry, University Science Books, Mill Valley, 1980.

5 G.W. Parshall, Chemical Society Specialist Periodical Report, Catalysis, 1 (1977) 335.

6 A.E. Shilov and A.A. Steinman, Coord. Chem. Rev., 24 (1977) 97.

7 D.E. Webster, Advan. Organometal. Chem., 15 (1977) 147.

8 P.J. Fagan, J.M. Manriquez, E.A. Maatta, A.M. Seyam and T.J. Marks, J. Amer. Chem. Soc., 103 (1981) 6650.

9 T.J. Marks and R.D. Ernst in G. Wilkinson, F.G.A. Stone, and E.W. Abel (Eds.), Comprehensive Organometallic Chemistry, Pergamon Press, Oxford, 1982, Chapt. 21.

10 For another case of where this type of process has been proposed for an organoactinide, see: S.J. Simpson, H.W. Turner, and R.A. Andersen, Inorg. Chem., 20 (1981) 2991.

11 J.W. Bruno, T.J. Marks, and V.W. Day, J. Amer. Chem. Soc., 104 (1982) 7357.

12 J.A. Ibers, R. DiCosimo, and G.M. Whitesides, Organometallics, 1 (1982) 13.

13 R. DiCosimo, S.S. Moore, A.F. Sowinski, and G.M. Whitesides, J. Amer. Chem. Soc., 104 (1982) 124, and references therein.

14 T.H. Tulip and D.L. Thorn, J. Amer. Chem. Soc., 103 (1981) 2448.

15 R.A. Jones and G. Wilkinson, J. Chem. Soc., Dalton Trans., (1979) 472.

16 R.A. Andersen, R.A. Jones, and G. Wilkinson, J. Chem. Soc., Dalton Trans., (1978) 446.

17 "International Tables for X-ray Crystallography", Kynoch Press, Birmingham, England, 1969, Vol. I, p. 99.

18 "International Tables for X-ray Crystallography", Kynoch Press, Birmingham, England, 1974, Vol. IV, pp. 55–66.

19 Ibid., pp. 99–101.

20 Ibid., pp. 149–150.

21 P.J. Fagan, J.M. Manriquez, S.H. Vollmer, C.S. Day, V.W. Day, and T.J. Marks, J. Amer. Chem. Soc., 103 (1981) 2206.

22 The R values are defined as $R_1 = \Sigma||F_0|-|F_c||/\Sigma|F_0|$ and $R_2 = \{\Sigma w(|F_0|-|F_c|)^2/\Sigma w|F_0|^2\}^{1/2}$, where w is the weight given each reflection. The function minimized is $\Sigma w(|F_0|-K|F_c|)^2$, where K is the scale factor.

23 Empirical weights were calculated from the equation $\sigma = \Sigma_0^3 a_n|F_0|^n = 5.06-(7.49\times10^{-2})|F_0|+(6.32\times10^{-4})|F_0|^2-(1.16\times10^{-6})|F_0|^3$, the a_n being coefficients derived from the least-squares fitting of the curve: $||F_0|-|F_c|| = \Sigma_0^3 a_n|F_0|^n$, where F_c values were calculated from the fully-refined model using unit weighting.

24 T.J. Marks, J.M. Manriquez, P.J. Fagan, V.W. Day, C.S. Day, and S.H. Vollmer, A.C.S. Sympos. Series, 131 (1980) 1.

25 Least-squares mean planes are defined by $-0.867x+0.494y+0.055z = 0.37$ for atoms C_{pa1}–C_{pa5}. x, y, z are orthogonal coordinates along $\vec{a}$, $\vec{b}$, and $\vec{c}^*$.

26 Least squares mean planes are defined by $-0.348x+0.735y+0.582z = 11.23$ for atoms C_{pb1}–C_{pb5}. x, y, and z are orthogonal coordinates along $\vec{a}$, $\vec{b}$, and $\vec{c}^*$.

27 The first number in parentheses following an averaged value of a bond length or angle is the root-mean-square estimated standard deviation of an individual datum. The second and third numbers, when given, are the average and maximum deviations from the averaged value, respectively. The fourth number represents the number of individual measurements which are included in the average value.

28 M.R. Churchill and R.W. Youngs, Inorg. Chem., 18 (1979) 1697.

29 M.R. Churchill and S.A. Julius, Inorg. Chem., 18 (1979) 2918.

30 D.P. Freyberg, J.L. Robbins, K.N. Raymond, and J.C. Smart, J. Amer. Chem. Soc., 101 (1979) 892.

31 P.J. Fagan, J.M. Manriquez, T.J. Marks, V.W. Day, S.H. Vollmer, and C.S. Day, J. Amer. Chem. Soc., 102 (1980) 5393.

32 J.M. Manriquez, P.J. Fagan, T.J. Marks, C.W. Day, and V.W. Day, J. Amer. Chem. Soc., 101 (1978) 7112.

33 R.W. Broach, A.J. Schultz, J.M. Williams, G.M. Brown, J.M. Manriquez, P.J. Fagan, and T.J. Marks, Science, 203 (1979) 172.

34 L. Pauling, The Nature of the Chemical Bond, 3rd ed., Cornell University Press, Ithaca, N.Y., 1960, p. 260.

35 Described by equation $-0.657x + 0.657y + 0.371z = 6.22$.

36 Described by equation $0.329x + 0.678y - 0.657z = 7.94$.

37 J.L. Petersen, C.L. Lichtenberger, R.F. Fenske, and L.F. Dahl, J. Amer. Chem. Soc., 97 (1975) 6433, and references therein.

38 K. Prout, T.S. Cameron, R.A. Forder, S.R. Critchley, B. Denton, and R.V. Rees, Acta Crystallogr. Sect. B., 30 (1974) 2290, and references therein.

39 V.W. Day and T.J. Marks, unpublished results.

40 G. Perego, M. Cesari, F. Farina, and G. Lugli, Acta Crystallogr., B32 (1976) 3034.

41 H. Schumann, W. Genthe, N. Bruncks, and J. Pickardt, Organometallics, 1 (1982) 1194.

42 This, however, is the preferred conformation in $Zr(C_5H_5)_2[CH_2Si(CH_3)_3]_2$ and $Zr(C_5H_5)_2[CH_2C(CH_3)_3]_2$: J. Jeffery, M.F. Lappert, N.T. Luong-Thi, M. Webb, J.L. Atwood, and W.E. Hunter, J. Chem. Soc., Dalton Trans., (1981) 1593.

43 L.E. Sutton (Ed.), Interatomic Distances, The Chemical Society, London, 1958; Supplement 1965.

44 N.L. Allinger et al., J. Amer. Chem. Soc., 90 (1968) 1199.

45 J.W. Bruno, C.W. Fendrick, and T.J. Marks, research in progress.